Mechanism of a Four-Phase Liquid Membrane Oscillator Containing Hexadecyltrimethylammonium Bromide

Maria Szpakowska,* Izabela Czaplicka, and Ottó B. Nagy

Gdañsk University of Technology, Faculty of Management and Economics, Commodity Science Laboratory, 80-952 GDANSK, Narutowicza str. 11/12, Poland

Received: December 16, 2005; In Final Form: March 9, 2006

The oscillatory behavior of a nitromethane based liquid membrane oscillator was investigated to contribute to the oscillation mechanism at the molecular level. At the beginning the system contains three phases: the aqueous donor phase in which the cationic surfactant, hexadecyltrimethylammonium bromide and ethanol are present and the aqueous acceptor phase made up by sucrose solution separated by the liquid membrane containing a constant amount of picric acid. During experiment a new phase x is created between the liquid membrane and acceptor phase. It was established that the oscillations take place at the membrane/phase x and the phase x/acceptor phase interfaces. Five basic regions can be distinguished in the oscillation pattern. The molecular events provoking the oscillations of electric potential difference between the two aqueous phases involve essentially the diffusion of hexadecyltrimethylammonium bromide and ion pairs formed by the cation of the surfactant and the picrate anion to the vicinity of the membrane/phase x interface, sudden adsorption of these ion pairs at this interface in noncatalytic and autocatalytic steps, desorption of ion pairs from the membrane/phase x interface into phase x, diffusion of ion pairs to the vicinity of phase x/acceptor phase interface, and sudden adsorption at this interface followed by desorption to the aqueous acceptor phase. It is shown by numerical simulations that the proposed mechanism may account for the observed oscillations and for the species distribution throughout the system as found experimentally. This four-phase system behaves like two coupled oscillators.

Introduction

Biologically important transport phenomena occur frequently in an oscillatory way (e.g., nerve impulses, cardiac and brain rhythms). Despite extensive studies on biooscillations[1,2] the physicochemical mechanisms of these phenomena are not yet known. Therefore, simpler artificial models have to be used for modeling such biological systems. Liquid membrane oscillators turn out to be a convenient tool for this purpose.

It was shown in previous publications[1−7] that nitrobenzene based liquid membrane oscillators containing cationic surfactants can mimic successfully the cellular behavior in taste sensing. Moreover, these systems might be used for molecular recognition of substances responsible for taste.[3−7] It was already established that oscillation characteristics change in a specific manner with the addition of various substances belonging to different taste categories. They were also sensitive to taste substance concentration.[3,5] Such systems were even proposed as a base for taste sensors.

In general, a liquid membrane oscillator is composed of two aqueous phases separated by an organic phase of different density (liquid membrane, m).[3−10] In the first aqueous phase (donor phase, d) surfactant is present that is transferred to the second aqueous phase (acceptor phase, a) through the liquid membrane (m) containing picric acid (HPi) dissolved in nitrobenzene or nitromethane. It was already found that the electric potential difference between the aqueous phases is changing in an oscillatory way.[3−9]

Although the detailed mechanism of these oscillations is still subject to controversy,[4,8,11−13] it was established previously[9] that when nitrobenzene was chosen as the liquid membrane solvent, the molecular events taking place at the membrane−aqueous acceptor phase interface (a/m) were responsible for the observed oscillations.

The detailed mechanism of nitrobenzene liquid membrane oscillators containing hexadecyltrimethylammonium bromide (HTMABr) has been described in ref 9. The proposed mechanism suggests that the sudden adsorption and desorption of surfactant molecules at the acceptor/membrane interface reinforced by the continuous feeding by diffusion is responsible for the observed oscillations.

As can be seen in this work, an interesting phenomenon occurs during the transport process when nitromethane is chosen as liquid membrane. A new phase (phase x) appears between the membrane and the aqueous acceptor phase creating thereby a four-phase system, which shows interesting mechanistic behavior. This system has more complex character than the nitrobenzene based oscillator[9] and therefore is better suited for modeling biological systems.

In the present work the influence of phase compositions of a nitromethane liquid membrane oscillator (initial HTMABr and HPi concentrations, pH of the aqueous phases) on oscillation characteristics has been investigated. A possible mechanism of oscillations of electric potential difference between the aqueous phases was proposed and confirmed by numerical simulations.

Experimental SectionPart

Reagents. HTMABr, ethanol, nitromethane, methanol, chloroform, sucrose, picric acid were commercial products of analytical grade purity (>99%). Stationary phase Diaion HPA25

* Corresponding author. E-mail: mszpak@pg.gda.pl.

10.1021/jp057349z CCC: $33.50
Published on Web 05/12/2006

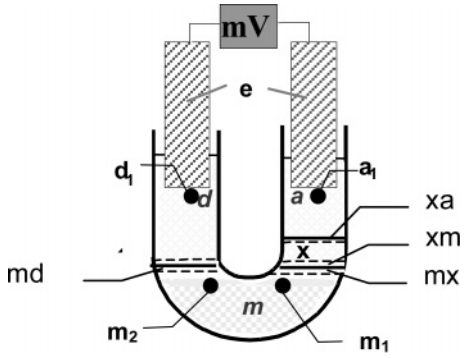

Figure 1. Experimental setup of liquid membrane oscillator. d_1, a_1, m_1, m_2: positions of electrodes in donor and acceptor aqueous phases and in liquid membrane, respectively. md, mx, xm and xa: layer in phase i in vicinity of phase j. e: $Ag/AgCl/Cl^-$ electrodes.

(Supelco) and disulfine blue (Fluka) were used in chromatography. HPi was recrystallized from an ethanol−water mixture (1:2 v/v) and nitromethane was distilled before use. Freshly distilled demineralized water was used in all experiments.

The experiments were performed in an apparatus with a U-shaped glass tube (12 mm inner diameter), Figure 1. Liquid membrane solution (m) was put at the bottom of the thermostated ($T = 25 \pm 0.1$ °C) U-tube. Above this layer an aqueous donor solution (d) and aqueous acceptor solution were introduced simultaneously. The initial composition of the three phases was the following:

(i) aqueous donor phase, 4 mL of 5×10^{-3} M HTMABr in ethanol (1.5 M)−water mixture

(ii) liquid membrane, 5 mL of 1.5×10^{-3} M HPi in nitromethane

(iii) aqueous acceptor phase, 4 mL of 0.1 M sucrose solution

The electric potential difference between the two aqueous phases (ΔE_{d1a1} in mV) was measured by using two $Ag/AgCl/Cl^-$ reference electrodes of 1.0 cm thickness situated at 1 cm (d_1, a_1) from the interfaces.

$\Delta E_{d_1/a_1}$ values were also measured by microelectrodes (0.1 cm thickness) situated 1 cm from interfaces in appropriate aqueous phases. In the membrane they were positioned as close as possible to the interfaces. In the case of interface potentials ($\Delta E_{d_1/m_2}$, $\Delta E_{a_1/m_1}$) a homemade microelectrode was used in the liquid membrane. This latter was made up of Ag/AgCl in contact with a solution of tetrabuthylammonium chloride (1.8×10^{-4} M) in nitromethane.

Each experiment was repeated four to six times. The obtained oscillation characteristics for each case were similar, never exactly the same. They were very sensitive to initial conditions (the way of interface preparation, temperature, electrode distances from interface). Particularly, the oscillation characteristics depend strongly on the topology of microelectrodes.[8,9] Therefore, all these parameters were kept constant and equal in each experiment.

The change of nitromethane concentrations in the two aqueous phases and phase x was measured using a Varian Cary 5E UV−vis−NIR spectrophotometer. The absorption band ($n-\pi^*$), at $\lambda_{max} = 269$ nm, $\epsilon_{max} = 14.4 \pm 0.1$ M^{-1} cm^{-1} (correlation coefficient = 0.991) for the donor phase and $\lambda_{max} = 267$ nm, $\epsilon_{max} = 13.8 \pm 0.1$ M^{-1} cm^{-1} (correlation coefficient = 0.993) for the acceptor and x phases was used in the calculation of appropriate concentrations. Similarly, the picric acid concentration was determined using the absorption at $\lambda_{max} = 355$ nm and $\epsilon_{max} = 13\,200 \pm 100$ M^{-1} cm^{-1} (correlation coefficient = 0.999).

Bromide ion concentration was established by microcoulometry using Analyzer multi X 2000 of Analytic Jena AG firm. Concentrations of HTMABr in aqueous acceptor phase and phase x were established using ion exchange chromatography followed by spectrophotometric measurements (HACH DR/2010).[14] pH values were measured using HaCH EC30 pH-meter. Numerical simulations were performed using Matlab program.

Results and Discussion

Immediately after the beginning of experiments (establishment of contacts between the membrane and aqueous phases), interesting new dynamic phenomena can be observed visually. The interface a/m becomes opaque and intensively yellow. A new transparent and colorless phase (x) appears between the membrane and this yellow stripe. The latter is diffusing into the acceptor phase where it disappears. The thickness of phase x is growing with time reaching its maximum (∼0.7 cm) around ∼1200 s. At the end of experiment (3600 s) phase x has a much smaller thickness. During these events hydrodynamic movements at the interfaces can be observed, which might be due to Marangoni effect.

By measuring electric potential differences in the various phases and also across the interfaces, we found that $\Delta E_{d_1/a_1}$ is composed of three contributions: (1) the potential difference across aqueous donor phase/membrane interface, $\Delta E_{d_1/m_2}$, (2) the diffusion potential difference in the liquid membrane, $\Delta E_{m_2/m_1}$, and (3) the potential difference across aqueous acceptor phase/membrane interface, $\Delta E_{m_1/a_1}$.

$$\Delta E_{d_1/a_1} = \Delta E_{d_1/m_2} + \Delta E_{m_2/m_1} + \Delta E_{m_1/a_1} \qquad (1)$$

This results from the fact that diffusion potentials inside two aqueous phases are close to zero. It should be noted that in the case of the nitrobenzene based oscillator diffusion potential in the membrane was also negligibly small.[9] Furthermore, the $\Delta E_{m_1/a_1}$ value is actually a composite quantity due to the appearance of a new phase x between the membrane and aqueous acceptor phase. Therefore, neglecting the diffusion potential in phase x, it can be written

$$\Delta E_{m_1/a_1} = -\Delta E_{a_1/m_1} = \Delta E_{m_1/x} + \Delta E_{x/a_1} \qquad (2)$$

The two components could not be measured for practical reasons (small thickness of the layer of phase x).

The appropriate changes of ΔE ($\Delta E_{d_1/a_1}$, $\Delta E_{a_1/m_1}$, $\Delta E_{d_1/m_2}$, and $\Delta E_{m_2/m_1}$) measured by means of microelectrodes are presented in Figure 2

After an initial period (∼800 s) oscillations of $\Delta E_{d_1/a_1}$ of different amplitudes and frequencies are observed (Figure 2a). In the case of $\Delta E_{a_1/m_1}$, oscillations begin only around 1600 s (Figure 2b) and they have phases opposite to the previous ones. There are no oscillations at the d/m interface (Figure 2c). However, $\Delta E_{d_1/m_2}$ values are diminishing with time in an irregular way. The much smaller initial $\Delta E_{m_2/m_1}$ value (∼25 mV) changes only slightly with time (Figure 2d).

The obtained results show clearly that the m/x and x/a interfaces are responsible for the oscillations of $\Delta E_{d_1/a_1}$. It should be noted that the influence of membrane thickness favors also these interfaces as the active site for oscillations.[8]

The contribution to $\Delta E_{d_1/a_1}$ values calculated from eq 1 at a certain process time are presented in Table 1.

It can be seen that the calculated $\Delta E_{d_1/a_1}$ values are in fairly good agreement with the experimental ones.

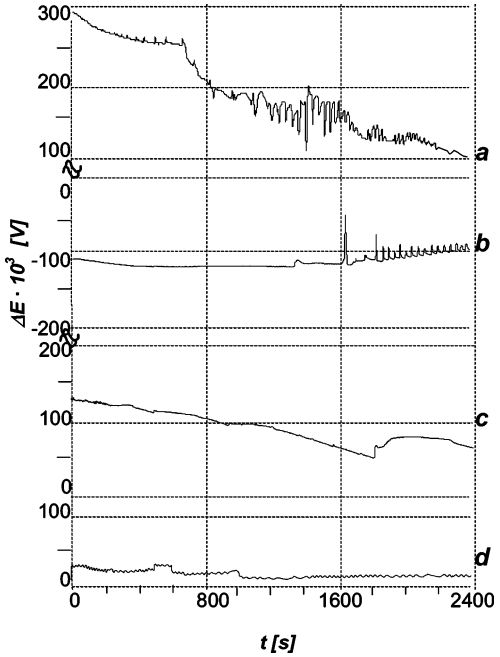

Figure 2. ΔE changes between appropriate phases measured by microelectrodes, (a) $\Delta E_{d_1/a_1}$, (b) $\Delta E_{a_1/m_1} = -(\Delta E_{m_1/x} + \Delta E_{x/a_1})$, (c) $\Delta E_{d_1/m_2}$, (d) $\Delta E_{m_2/m_1}$.

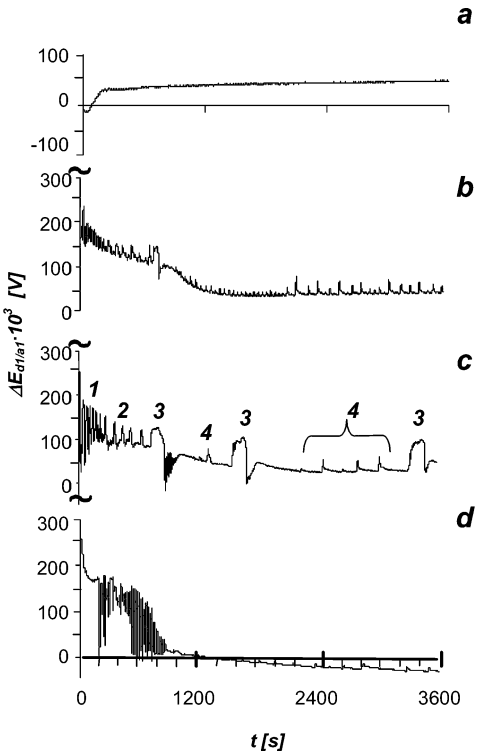

Figure 3. Influence of initial HTMABr concentration in donor phase on the oscillation curves: (a) 0 M;[15] (b) 3×10^{-3} M; (c) 5×10^{-3} M; (d) 10^{-2} M.

TABLE 1: Components of the Observed Electric Potential Difference ($\times 10^{-3}$ V) between the Aqueous Phases

t (s)	$\Delta E_{d_1/m_2}$	$\Delta E_{m_2/m_1}$	$\Delta E_{a_1/m_1}$	$\Delta E_{d_1/a_1}$ calculated	$\Delta E_{d_1/a_1}$ experimental
0	125	25	−110	260	275
800	110	10	−120	240	220
1600	70	10	−120	200	180
2400	70	10	−100	180	160

The oscillation curves of $\Delta E_{d_1/a_1}$ at different initial surfactant concentrations are presented in Figure 3. They were measured by thick electrodes (see experimental part).

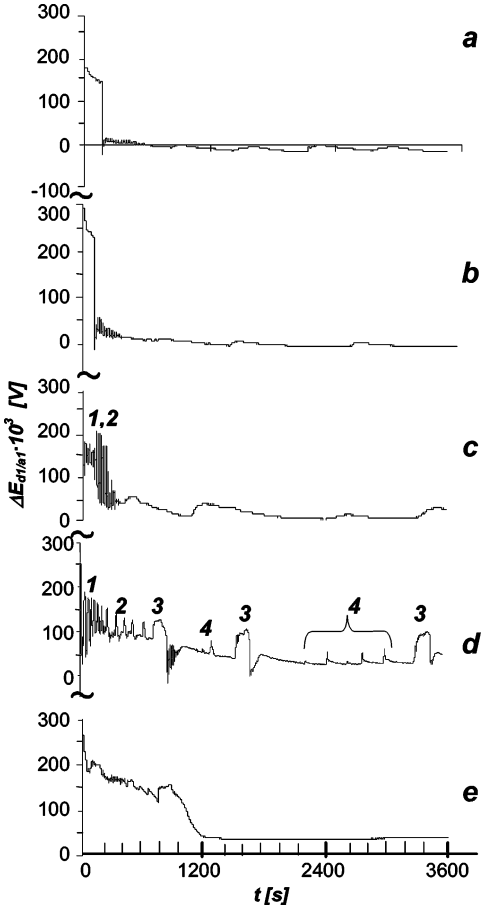

Figure 4. Influence of initial HPi concentration in liquid membrane on $\Delta E_{d1/a1}$ curves: (a) 0 M ;[9] (b) 0.3×10^{-3} M; (c) 1.2×10^{-3} M; (d) 1.5×10^{-3} M; (e) 3×10^{-3} M.

It can be seen that the type of oscillations and their characteristics (frequency, amplitude and phase) are very sensitive to the initial amount of surfactant present in the donor phase. In the absence of surfactant no oscillations are observed (Figure 3a). When the surfactant concentration is close to its critical micelle concentration value, cmc (cmc = 1.15×10^{-3} M for HTMABr measured in ethanol (1.5 M)−water mixture), small amplitude oscillations of different frequencies appear without induction period, separated by a wide peak (Figure 3b). When the surfactant concentration is about 5 times higher than the cmc value, peaks of four different types are observed (Figure 3c). High-frequency oscillations appear at the beginning (no. 1) followed by lower frequency oscillations (no. 2). After this period, wider peaks of different phases appear (no. 3). They are surrounded by small amplitude and small frequency oscillations (no. 4). This type of peak is observed also in the absence of alcohol.[9,15] At even higher surfactant concentrations only high-frequency oscillations can be observed at the beginning of the transport process following an induction period (Figure 3d). The initial surfactant concentration of 5×10^{-3} M was chosen for further experiments on account of the large variety of peaks observed.

The influence of initial HPi concentration is presented in Figure 4.

No oscillations are observed in absence of HPi (Figure 4a). Increasing the concentration of the latter peaks of type 1 and 2 appear followed by peaks of type 3 throughout the experiment (Figure 4c). All four types of peaks are observed at higher concentrations (Figure 4d). When the concentration is further

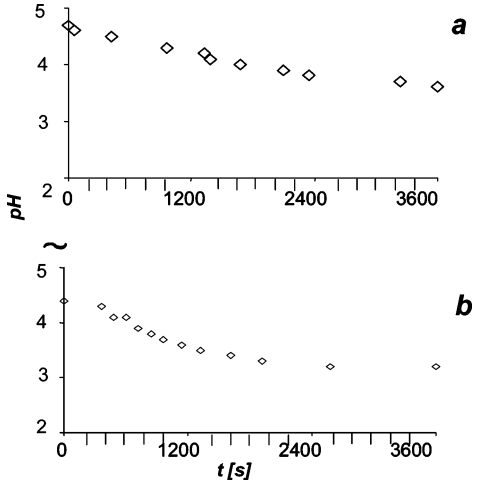

Figure 5. pH changes in (a) donor phase and (b) acceptor phase during oscillation process.

TABLE 2: Composition of the Various Phases of Oscillator with HTMABr before and at the End of Experiment

	concn [M] × 10^3					
	donor phase		acceptor phase		phase x[b]	
substance	initial	final	initial	final	initial	final
nitromethane	0	131	0	251	lack of phase x	800−1000
H^+ [a]	∼0	0.25	0.02	0.50		1
Pi^-	0	0	0	0.073		∼0
$HTMA^+$	5		0	0.001		0.002
Br^-	5	4.5	0	0.12		1.5

[a] Calculated from pH. [b] After 1800 s.

increased, irregular oscillations are observed only at the beginning of the experiment.

The diffusion of nitromethane and HPi into the two aqueous phases provokes a significant changes of their acidity (pK_a (HPi) = 0.25; pK_a (nitromethane) = 10.2 [16]). The time evolutions of the pH of various phases are presented in Figure 5.

It can be seen that the pH of the donor phase decreases monotonically with time. This decrease is more significant for the acceptor phase.

The distributions of various species in the two aqueous phases and in phase x as found before and at the end of experiment are presented in Table 2.

It can be seen that final compositions of the two aqueous phases are significantly different from their initial values. Nitromethane diffuses into both aqueous phases during the experiments. As a result, the phases become more acid. It should be noted that nitromethane is transferred to the aqueous phases mainly in the first 180 s of the process and its concentration remains virtually constant afterward.

Picrate ions were observed only in the acceptor phase at the end of experiment. Surfactant cations and bromide ions are transferred from the donor to the acceptor phase. It should be noted that the amount of transferred bromide ions is much higher than that of surfactant cations.

The new phase x deserves special mention because it is not present at the beginning of the experiment and it diminishes significantly at the end. Therefore, the final concentration values were established at 1800 s. It can be seen that this phase is very rich in nitromethane. Its acidity is relatively high compared to the aqueous phases. Also the concentration of surfactant cations and bromide ions is much higher than in the acceptor phase. It should be noted that the appearance of phase x is

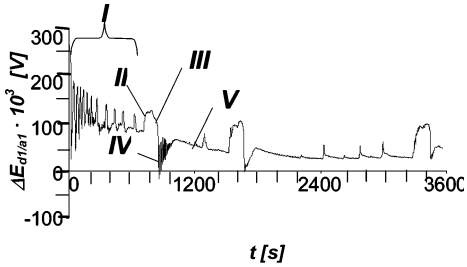

Figure 6. Different regions in oscillation pattern of nitromethane liquid membrane oscillator containing HTMABr.

accompanied by the creation of the first large oscillation peak (no. 3 in Figure 3c).

Figure 6 suggests that five basic regions can be distinguished in the oscillation pattern:

I, region of appearance of high-frequency peaks (nos. 1 and 2 in Figure 3c)

II, first large peak (no. 3) formation (increase of $\Delta E_{d_1/a_1}$ values)

III, creation of the first large peak (decrease of $\Delta E_{d_1/a_1}$ values)

IV, increase of $\Delta E_{d_1/a_1}$ in a rapidly oscillating way

V, region without oscillations

Regions II−V are repeated, giving rise to the observed oscillation peaks no. 3.

The following molecular events may take part in the oscillation process.

At the beginning interface d/m is populated by $HTMA^+$ cations. They are exchanged at this interface with H^+ cations from picric acid present in the liquid membrane, making the donor phase more acid. This leads also to the formation of surfactant−picrate ion pairs in the vicinity of d/m interface ($HTMAPi_{md}$). Nitromethane is rapidly transferred into the donor phase due to its high solubility in water (8.7% w/w at $T = 25$ °C[16]). This contributes also to the total acidity increase. Actually, nitromethane transfer to both aqueous phases takes place already at the very beginning in a violent way. Both diffusion and hydrodynamic movements due to the Marangoni effect are responsible for this transfer. As a result, surfactant molecules are present at the a/m interface from the first moment, as shown by the significant drop of the initial electric potential difference between the aqueous phases ($\Delta E^0_{d_1/a_1}$). It is followed by rapid oscillations due to adsorption/desorption processes taking place at the a/m interface (region I). $HTMAPi_{md}$ and surfactant molecules in the vicinity of d/m interface, $HTMABr_{md}$, diffuse across the membrane from the proximity of d/m interface (md) to the vicinity of m/x interface (mx) (eqs 3 and 4). It should be noted that another possible source of $HTMAPi_{mx}$ is supplied by the exchange process as shown by eq 8.

$HTMAPi_{mx}$ and $HTMABr_{mx}$ being in the vicinity of the m/x interface adsorbs suddenly to this interface in an uncatalyzed (eqs 5 and 6) and autocatalyzed way (eq 7). These processes cause $\Delta E_{d_1/a_1}$ values to decrease (region III).

HTMAPiI and HTMABrI ion pairs present at the m/x interface, I designating the sites occupied by the ion pairs, desorb into phase x (eqs 9 and 10). As a result, the $\Delta E_{d_1/a_1}$ value increases (region II).

In phase x similar processes take place as in the membrane phase (eqs 11−16). S designates the sites occupied by the surfactant cation at the x/a interface. It is supposed that surfactant is adsorbed in ionic form due to the higher polarity of the interface x/a.

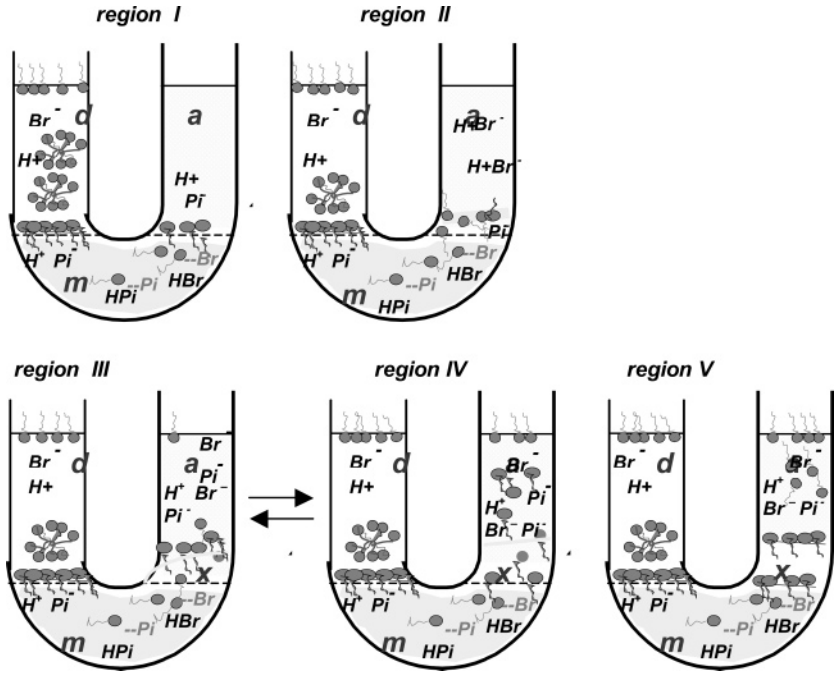

Figure 7. Oscillation mechanism in the nitromethane oscillator containing HTMABr (● $HTMA^+$ ion).

These molecular events involved in the oscillation mechanism are summarized by eqs 3−16 and Figure 7.

$$\mathrm{HTMAPi_{md}} \xrightarrow{k_1} \mathrm{HTMAPi_{mx}} \quad (3)$$

$$\mathrm{HTMABr_{md}} \xrightarrow{k_2} \mathrm{HTMABr_{mx}} \quad (4)$$

$$\mathrm{HTMAPi_{mx}} + I \xrightarrow{k_3} \mathrm{HTMAPiI} \quad (5)$$

$$\mathrm{HTMABr_{mx}} + I \xrightarrow{k_4} \mathrm{HTMABrI} \quad (6)$$

$$\mathrm{HTMAPi_{mx}} + \mathrm{I} + \mathrm{HTMAPiI} \xrightarrow{k_5} 2\mathrm{HTMAPiI} \quad (7)$$

$$\mathrm{HTMABr_{mx}} + \mathrm{HPi_m} \xrightarrow{k_6} \mathrm{HBr_x} + \mathrm{HTMAPi_{mx}} \quad (8)$$

$$\mathrm{HTMAPiI} \xrightarrow{k_7} \mathrm{HTMAPi_{xm}} + \mathrm{I} \quad (9)$$

$$\mathrm{HTMABrI} \xrightarrow{k_8} \mathrm{HTMABr_{xm}} + \mathrm{I} \quad (10)$$

$$\mathrm{HTMAPi_{xm}} \xrightarrow{k_9} \mathrm{HTMAPi_{xa}} \quad (11)$$

$$\mathrm{HTMABr_{xm}} \xrightarrow{k_{10}} \mathrm{HTMABr_{xa}} \quad (12)$$

$$\mathrm{HTMAPi_{xa}} + \mathrm{S} \xrightarrow{k_{11}} \mathrm{HTMA^+S} + \mathrm{Pi_a^-} \quad (13)$$

$$\mathrm{HTMABr_{xa}} + \mathrm{S} \xrightarrow{k_{12}} \mathrm{HTMA^+S} + \mathrm{Br_a^-} \quad (14)$$

$$\mathrm{HTMAPi_{xa}} + \mathrm{S} + \mathrm{HTMA^+S} \xrightarrow{k_{13}} 2\mathrm{HTMA^+S} + \mathrm{Pi_a^-} \quad (15)$$

$$\mathrm{HTMA^+S} \xrightarrow{k_{14}} \mathrm{HTMA_a^+} + \mathrm{S} \quad (16)$$

The reverse reactions of each step are neglected to simplify the mathematical analysis. In establishing these equations, we consider the various molecules situated in different environments as different species.[9] It is also admitted that the interface x/a has a larger thickness than the interface m/x, and consequently, the amount of sites present in the former is kept constant (S_0).

By applying the laws of chemical kinetics to the various species involved,[9] we obtained the following system of differential equations:

$$\frac{\mathrm{d[HTMAPi_{mx}]}}{\mathrm{d}t} = k_1[\mathrm{HTMAPi_{md}}]_0 + k_6[\mathrm{HTMABr_{mx}}][\mathrm{HPi_m}] - k_3[\mathrm{HTMAPi_{mx}}][\mathrm{I}] - k_5[\mathrm{HTMAPi_{mx}}][\mathrm{I}][\mathrm{HTMAPiI}] \quad (17)$$

$$\frac{\mathrm{d[HTMABr_{mx}]}}{\mathrm{d}t} = k_2[\mathrm{HTMABr_{md}}]_0 - k_4[\mathrm{HTMABr_{mx}}][\mathrm{I}] - k_6[\mathrm{HTMABr_{mx}}][\mathrm{HPi_m}] \quad (18)$$

$$\frac{\mathrm{d[HTMAPiI]}}{\mathrm{d}t} = k_3[\mathrm{HTMAPi_{mx}}][\mathrm{I}] + k_5[\mathrm{HTMAPi_{mx}}][\mathrm{I}][\mathrm{HTMAPiI}] - k_7[\mathrm{HTMAPiI}] \quad (19)$$

$$\frac{\mathrm{d[I]}}{\mathrm{d}t} = -k_3[\mathrm{HTMAPi_{mx}}][\mathrm{I}] - k_4[\mathrm{HTMABr_{mx}}][\mathrm{I}] - k_5[\mathrm{HTMAPi_{mx}}][\mathrm{I}][\mathrm{HTMAPiI}] + k_7[\mathrm{HTMAPiI}] + k_8[\mathrm{HTMABrI}] \quad (20)$$

$$\frac{d[HTMAPi_{xm}]}{dt} = k_7[HTMAPiI] - k_9[HTMAPi_{xm}] \quad (22)$$

$$\frac{d[HTMABr_{xm}]}{dt} = k_8[HTMABrI] - k_{10}[HTMABr_{xm}] \quad (23)$$

$$\frac{d[HTMAPi_{xa}]}{dt} = k_9[HTMAPi_{xm}] - k_{11}[HTMAPi_{xa}][S_0] - k_{13}[HTMAPi_{xa}][S_0][HTMA^+S] \quad (24)$$

$$\frac{d[HTMA^+S]}{dt} = k_{11}[HTMAPi_{xa}][S_0] + k_{12}[HTMABr_{xa}][S_0] + k_{13}[HTMAPi_{xa}][S_0][HTMA^+S] - k_{14}[HTMA^+S] \quad (25)$$

$$\frac{d[HTMABr_{xa}]}{dt} = k_{10}[HTMABr_{xm}] - k_{12}[HTMABr_{xa}][S_0] \quad (26)$$

These are nonlinear equations having unknown rate constants and concentrations of different species. They have been used to verify the possibility of oscillations.

The species in vicinity of the d/m interface, $HTMAPi_{md}$ and $HTMABr_{md}$, are considered to be in the steady state. Therefore, their initial concentrations were taken at the constant values of $[HTMAPi_{md}]_0 = 5 \times 10^{-5}$ M and $[HTMABr_{md}]_0 = 10^{-5}$ M. This is a generally used approach to simplify the rather complicated kinetic scheme. The large excess of picric acid in the membrane, $[HPi_m] = 10^{-3}$ M, is also considered constant. The initial concentrations of the sites present in the interfaces, I_0 and S_0, are both estimated to 10^{-5} M by using molecular dimensions of adsorbing species. The various rate constants used in the calculations are the following: $k_1 = 10^{-3}$ [s^{-1}], $k_2 = 2 \times 10^{-3}$ [s^{-1}], $k_3 = 10^5$ [M^{-1} s^{-1}], $k_4 = 10^5$ [M^{-1} s^{-1}], $k_5 = 10^6$ [M^{-2} s^{-1}], $k_6 = 10$ [M^{-1} s^{-1}], $k_7 = 1$ [s^{-1}], $k_8 = 1$ [s^{-1}], $k_9 = 5 \times 10^{-3}$ [s^{-1}], $k_{10} = 8 \times 10^{-3}$ [s^{-1}], $k_{11} = 10^5$ [M^{-1} s^{-1}], $k_{12} = 10^5$ [M^{-1} s^{-1}], $k_{13} = 10^6$ [M^{-2} s^{-1}] and $k_{14} = 10^{-2}$ [s^{-1}].

The choice of the relative values of the rate constants is based on the following considerations. It is admitted that the slow diffusion across the membrane and phase x is followed by fast adsorption into the appropriate interface and a much slower desorption into the next phase (phase x and a).

Therefore, k_1 is chosen smaller than k_2 and k_9 smaller than k_{10} because the ion pairs containing the picrate ions diffuse more slowly than HTMABr due to their greater size. It is assumed that the adsorption processes have the same rate for both ion pairs ($k_3 = k_4$ and $k_{11} = k_{12}$). The rate of the autocatalytic step is considered faster than the corresponding noncatalytic one ($k_5 > k_3$ and $k_{13} > k_{11}$). The desorption processes are considered to be slower than the adsorptions to the interface (k_7, k_8, $k_{14} < k_3$, k_4, k_5, k_{11}, k_{12}, k_{13}). The actual numerical values for the rate constants were determined by their ability to produce oscillations in the numerical experimentation.

The obtained results for $HTMAPi_{mx}$ and $HTMAPi_{xa}$ are represented in Figure 8. It can be seen that these species present

$$\frac{d[HTMABrI]}{dt} = k_4[HTMABr_{mx}][I] - k_8[HTMABrI] \quad (21)$$

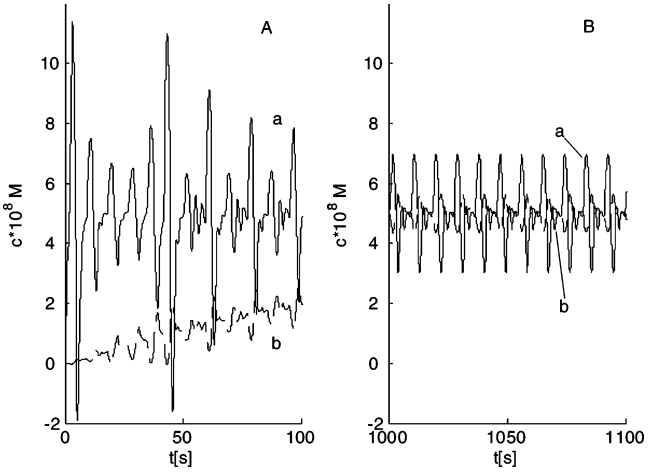

Figure 8. Numerical simulation of oscillatory behavior of the concentrations of $HTMAPi_{mx}$ (a) and of $HTMAPi_{xa}$ (b) in the 0−100 s process time (A) and in the 1000−1100 s process time (B).

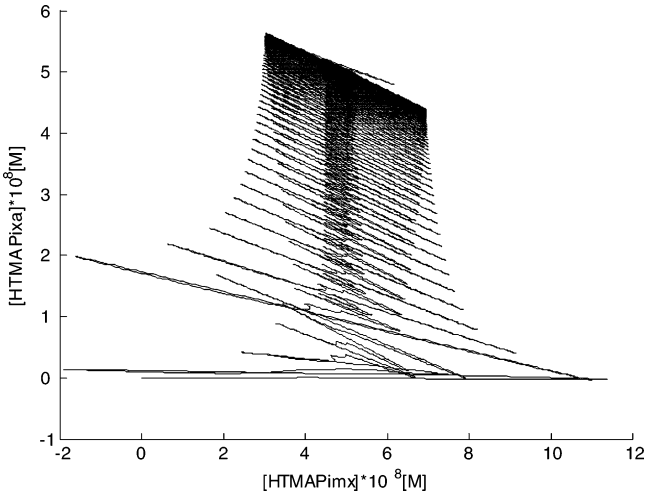

Figure 9. Phase portrait of the nitromethane oscillator based on the changes of the concentrations of two species $HTMAPi_{xa}$ and $HTMAPi_{mx}$ in the range 0−1100 s.

irregular oscillations. Both oscillations show chaotic character. However, the oscillations taking place in the membrane (Figure 8, curve a) have larger amplitudes than those occurring in phase x (Figure 8, curve b). The other species show similar behavior with the exception of $HTMA^+S$ whose concentration does not oscillate with time.

The dynamical behavior of the system can be followed by means of two-dimensional phase portraits.[9] The phase portrait obtained for the two oscillating species of Figure 8 in the range 0−1100 s is given in Figure 9. The $HTMAPi_{mx}$ concentration starting from 0 reaches a significant value before $HTMAPi_{xa}$ appears in phase x at the proximity of the x/a interface. This initial phase is followed by chaotic oscillations which became after more regular.

All these results obtained by numerical simulations suggest that the proposed mechanism may account for the observed oscillations and also for the chemical compositions of the different phases as presented in Table 2. Similarly to the nitrobenzene liquid membrane oscillator,[9] the following points can be stressed: (a) acidification of aqueous phases during oscillation process, (b) excess of bromide ions in comparison to surfactant cations in the acceptor phase, (c) presence of Pi^- ions in the acceptor phase, and (d) small amount of $HTMA^+$ cations in acceptor phase.

The appearance of phase x during the experiment transforms the initial three-phase system into a four-phase one. The oscillations take place in the second (membrane) and the third (phase x) phase. Therefore, the whole system can be considered as composed of two coupled oscillators. The oscillations in the membrane induce through coupling oscillations in phase x but of smaller amplitude. This situation may resemble the transmission of excitations among cells in living organism.

Conclusion

The nitromethane liquid membrane oscillator with HTMABr is a four-phase system in which the oscillations take place at the membrane/phase x (m/x) and phase x/acceptor phase (x/a) interfaces. The appearance of significant oscillations requires the simultaneous presence of cationic surfactant, picric acid and ethanol in the system.

The proposed mechanism suggests that the sudden adsorption and desorption of surfactant molecules at interfaces m/x and x/a reinforced by the continuous feeding by diffusion is responsible for the observed oscillations of electric potential difference between the donor and acceptor aqueous phases. The set of nonlinear differential equations describing the time evolution of the various chemical species involved in the mechanism can account for the observed oscillations and for the species distribution across the system. The dynamics of the system is chaotic, as shown by the attractors obtained in two-dimensional phase space.

References and Notes

(1) Larter, R. *Chem. Rev.* **1990**, 355−381.

(2) Rastogi, R. P.; Srivastava, R. C. *Adv. Colloid Interface Sci.* **2001**, 93, 1−75.

(3) Szpakowska, M.; Płcharska-Jankowska, E.; B. Nagy, O. *Desalination* **2005**, 173, 61−67.

(4) Yoshikawa, K.; Omochi, T.; Matsubara, Y. *Biophys. Chem.* **1986**, *23*, 211−214.

(5) Szpakowska, M.; Magnuszewska, A.; Szwacki, J. *J. Membr. Sci.* **2006**, *273*, 116−123.

(6) Płocharska-Jankowska, E.; Szpakowska, M.; Mátéfi-Tempfli, S.; B. Nagy, O. *Biophys. Chem.* **2005**, *114*, 85−93.

(7) Yoshikawa, K.; Shoji, M.; Nakata, S.; Maeda, S.; Kawakami, H. *Langmuir* **1988**, *4*, 759−762.

(8) Szpakowska, M.; Czaplicka, I.; Płocharska-Jankowska, E.; B. Nagy, O. *J. Colloid Interface Sci.* **2003**, *261*, 451−455.

(9) Szpakowska, M.; Czaplicka, I.; B. Nagy, O. *Biophys. Chem.* **2006**, *120*, 148−153.

(10) Szpakowska, M.; Czaplicka, I. *Ars Sep. Acta* **2003**, *2*, 64−70.

(11) Arai, K.; Kusu, F.; Takamura, K. *Chem. Lett.* **1990**, 1517−1520.

(12) Maeda, K.; Nagami, S.; Yoshida, Y.; Ohde, H.; Kihara, S. *J. Electroanal. Chem.* **2001**, *496*, 124−130.

(13) Pimienta, V.; Etchenique, R.; Buhse, T. *J. Phys. Chem. A* **2001**, *105*, 10037−10044.

(14) Sheiham, I.; Pinfold, T. A. *Analyst* **1969**, *94*, 387−388.

(15) Szpakowska, M.; Czaplicka, I.; Szwacki, J.; B. Nagy, O. *Chem. Pap.* **2002**, *56*, 20−24.

(16) Weast, R. C., Astle, M. J., Eds. *Handbook of Chemistry and Physics*; CRC Press: Boca Raton, FL, 2000.